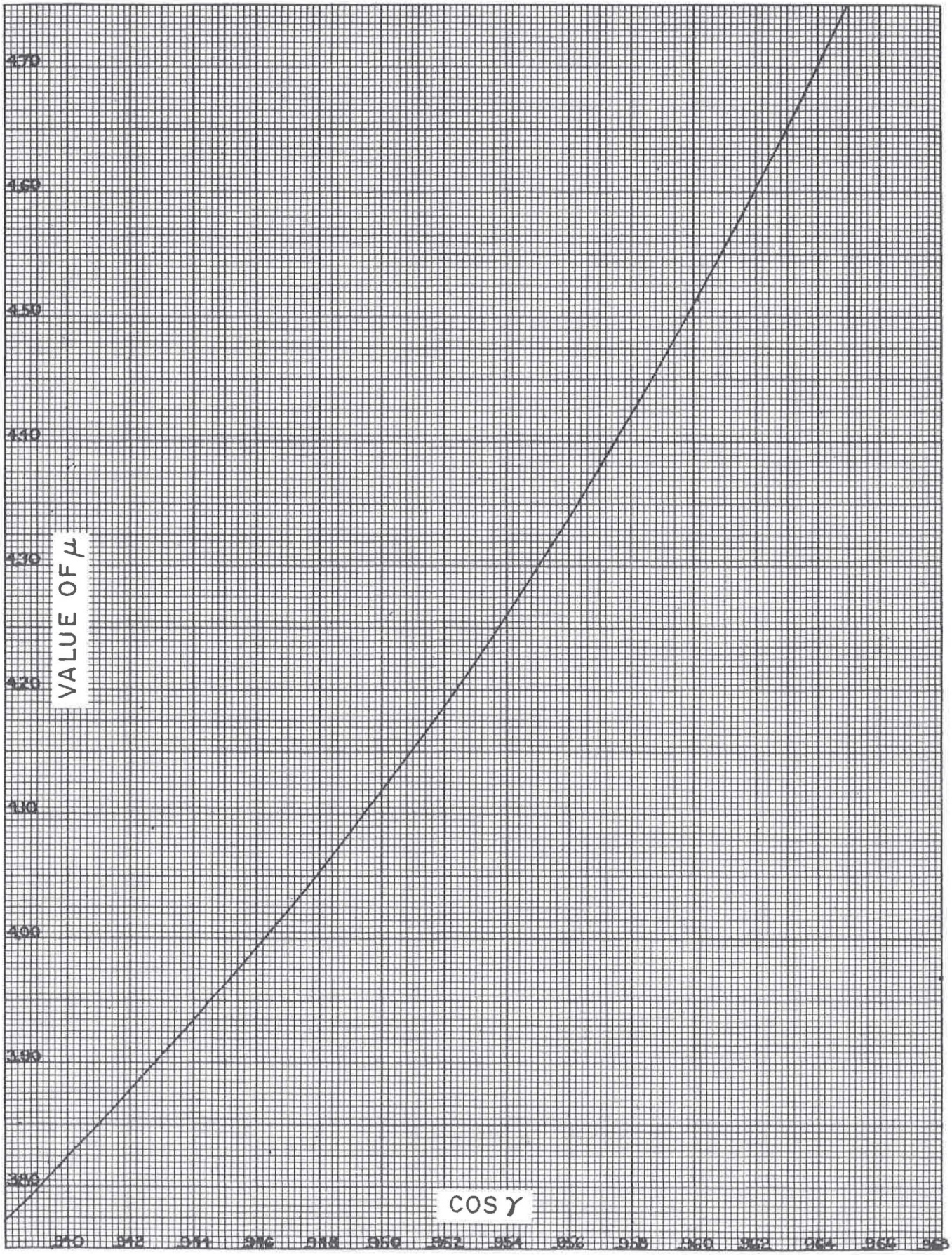
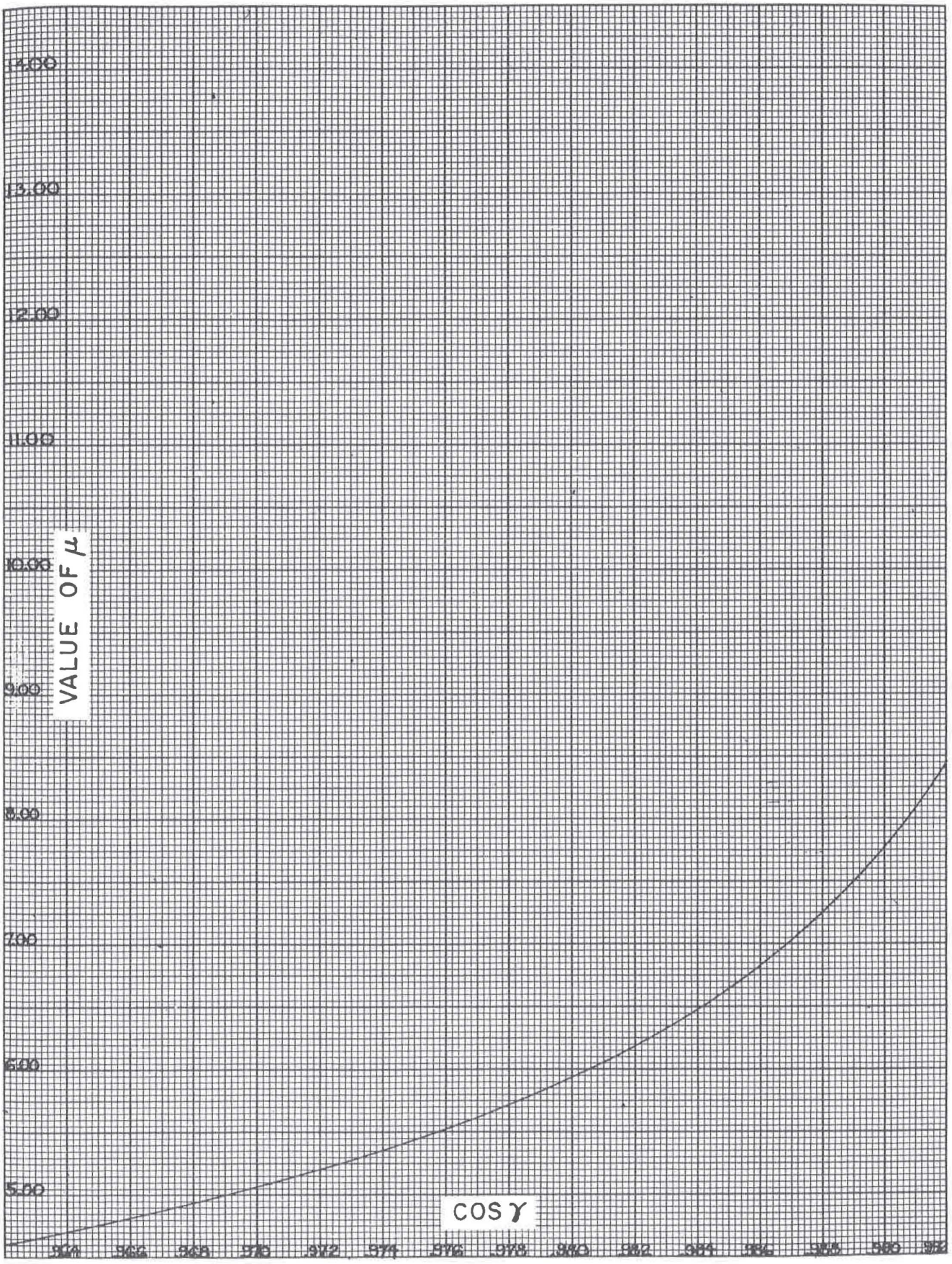
Chart A-14

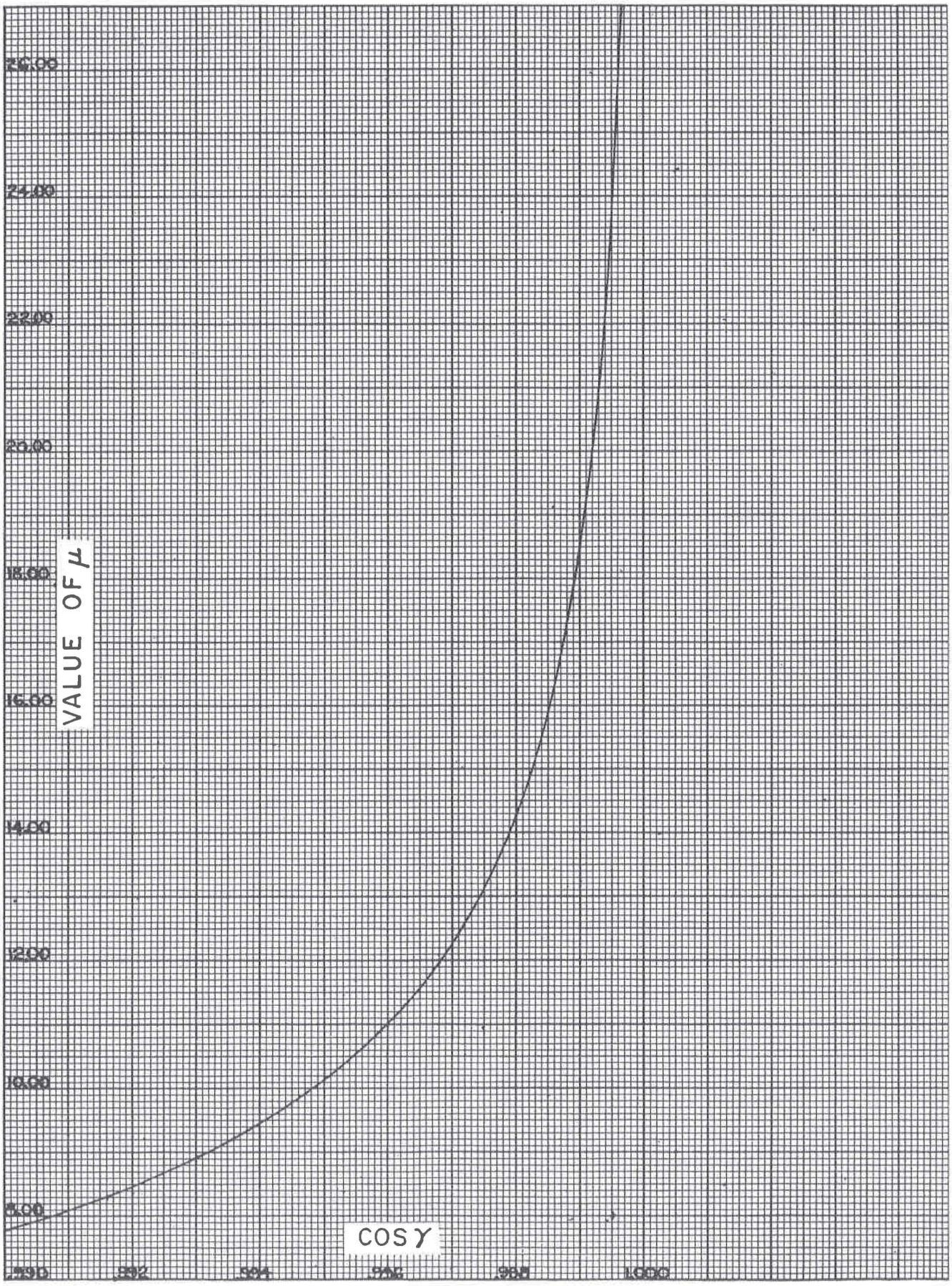


American Axle v. Neapco - IPR2025-00091
PET_AAM_1012-0368



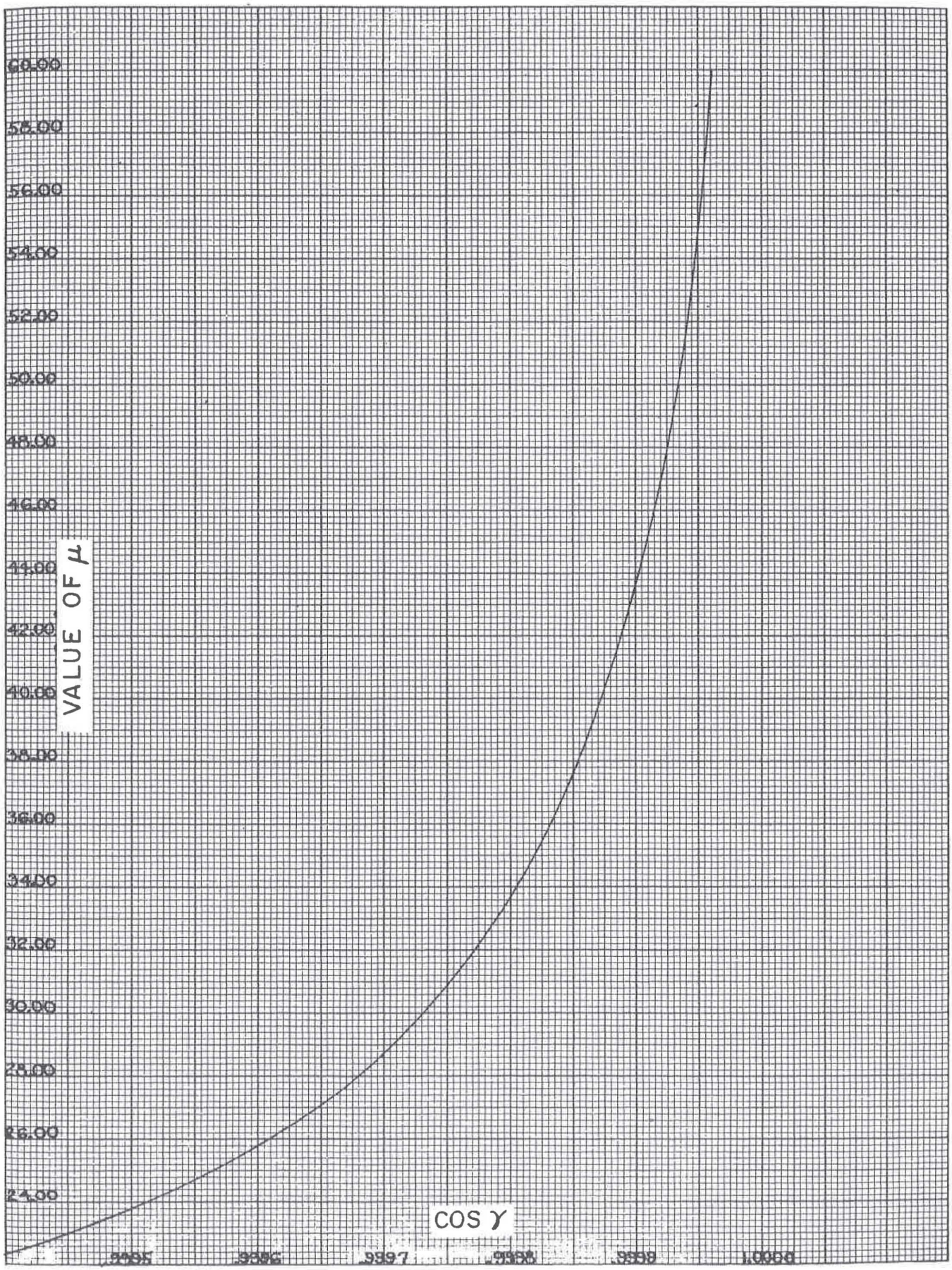
American Axle v. Neapco - IPR2025-00091
PET_AAM_1012-0369

Chart A-16



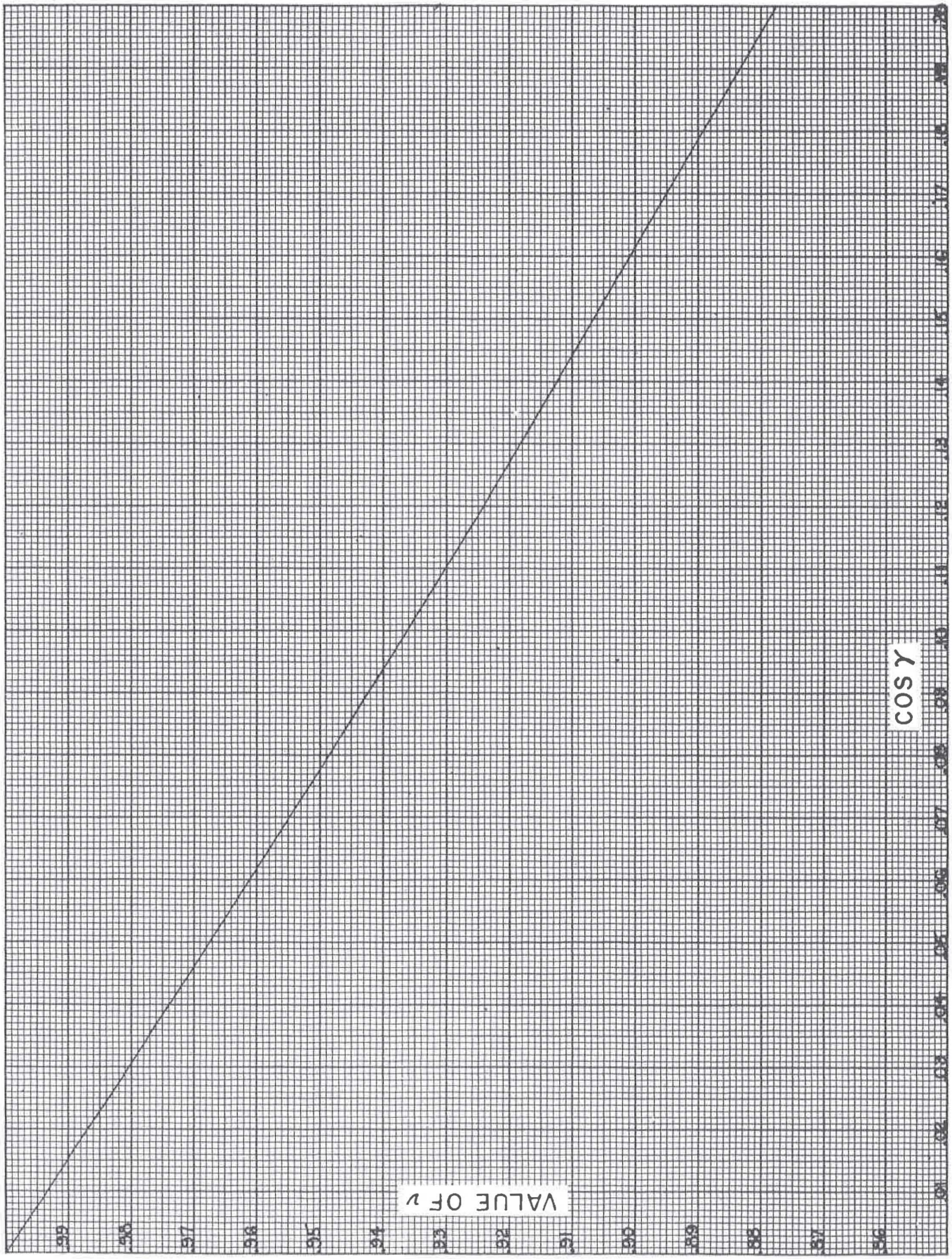
American Axle v. Neapco - IPR2025-00091
PET_AAM_1012-0370

Chart A-17

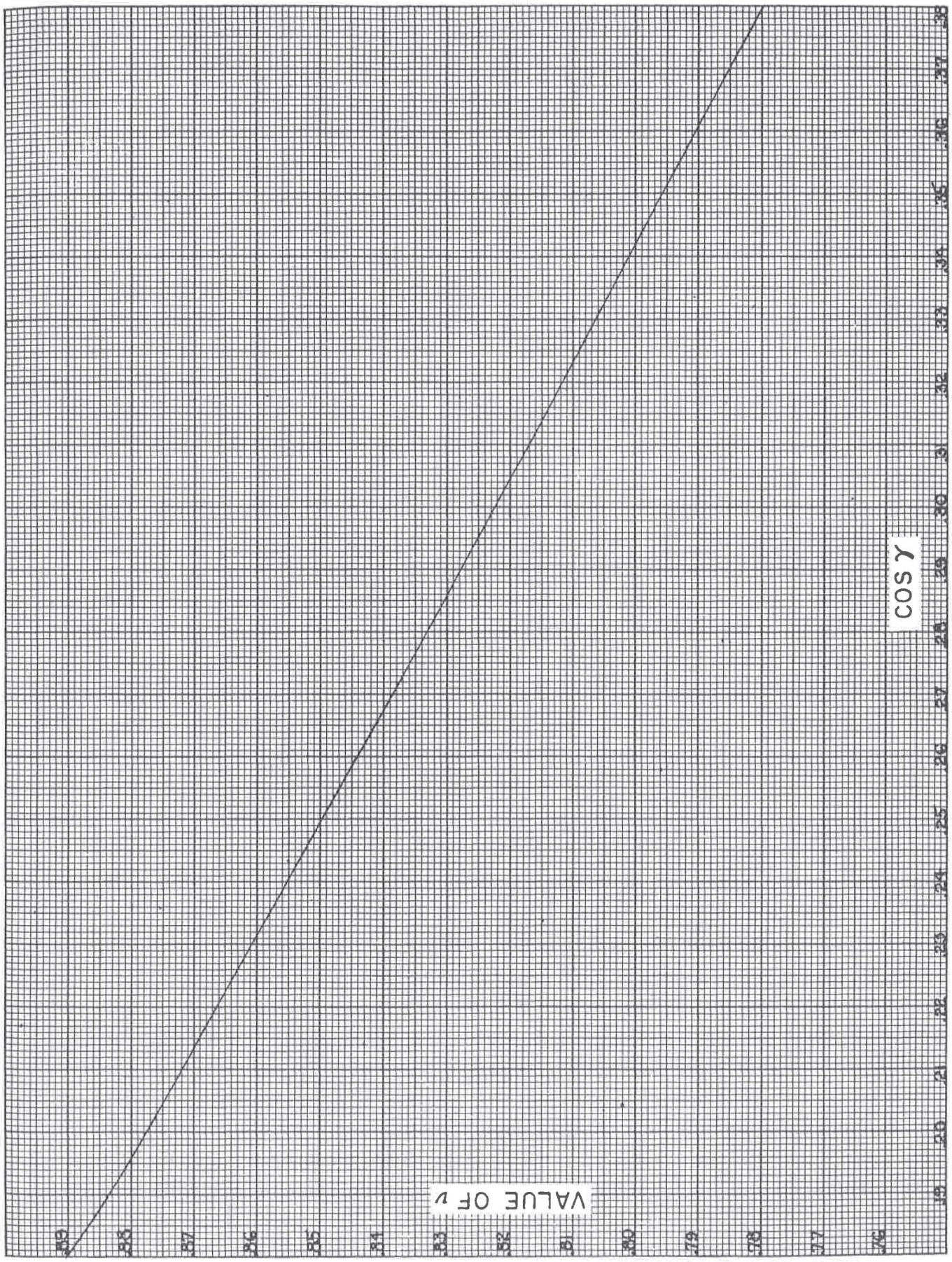


American Axle v. Neapco - IPR2025-00091
PET_AAM_1012-0371

Chart A-18

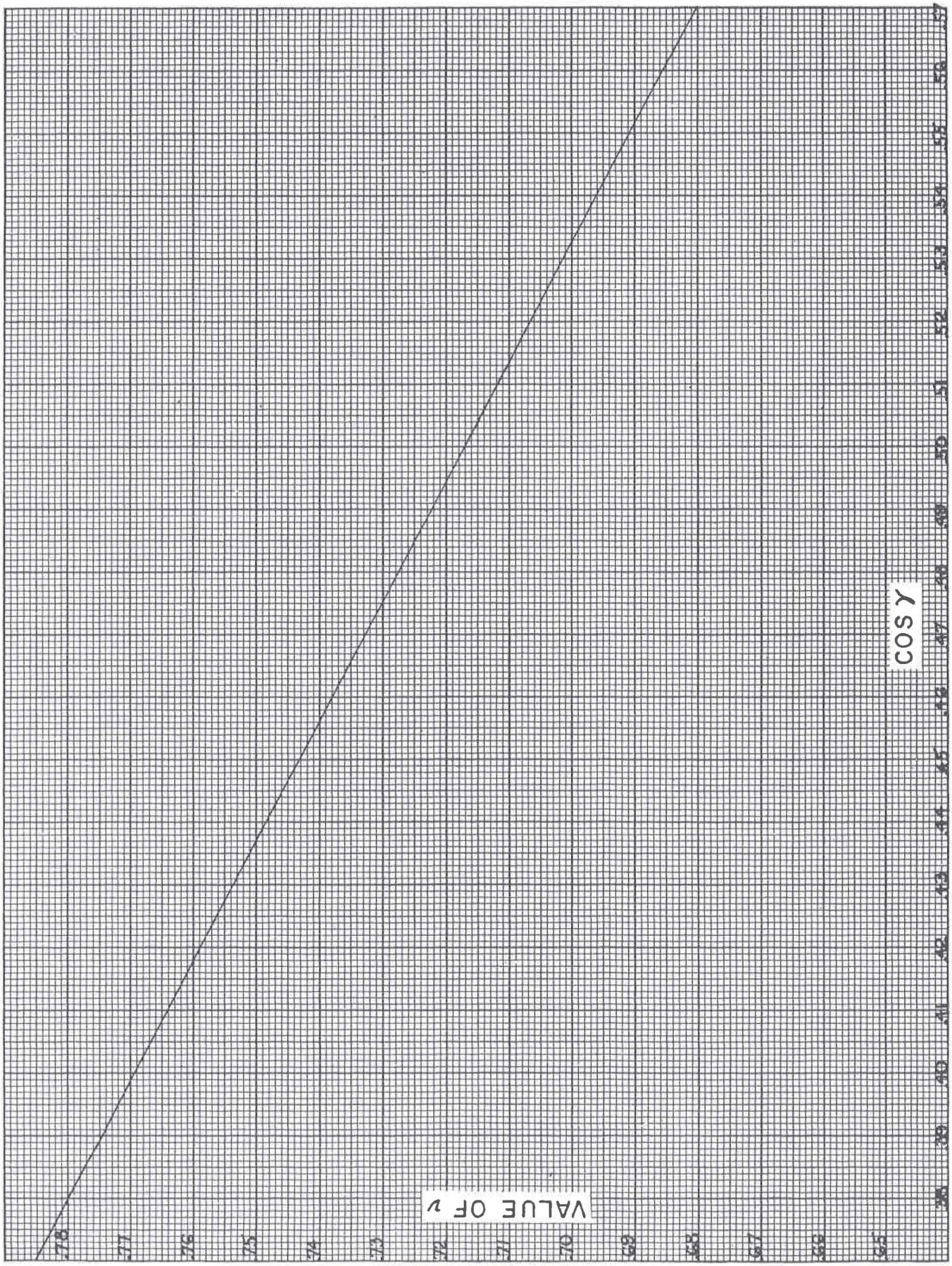


American Axle v. Neapco - IPR2025-00091
PET_AAM_1012-0372

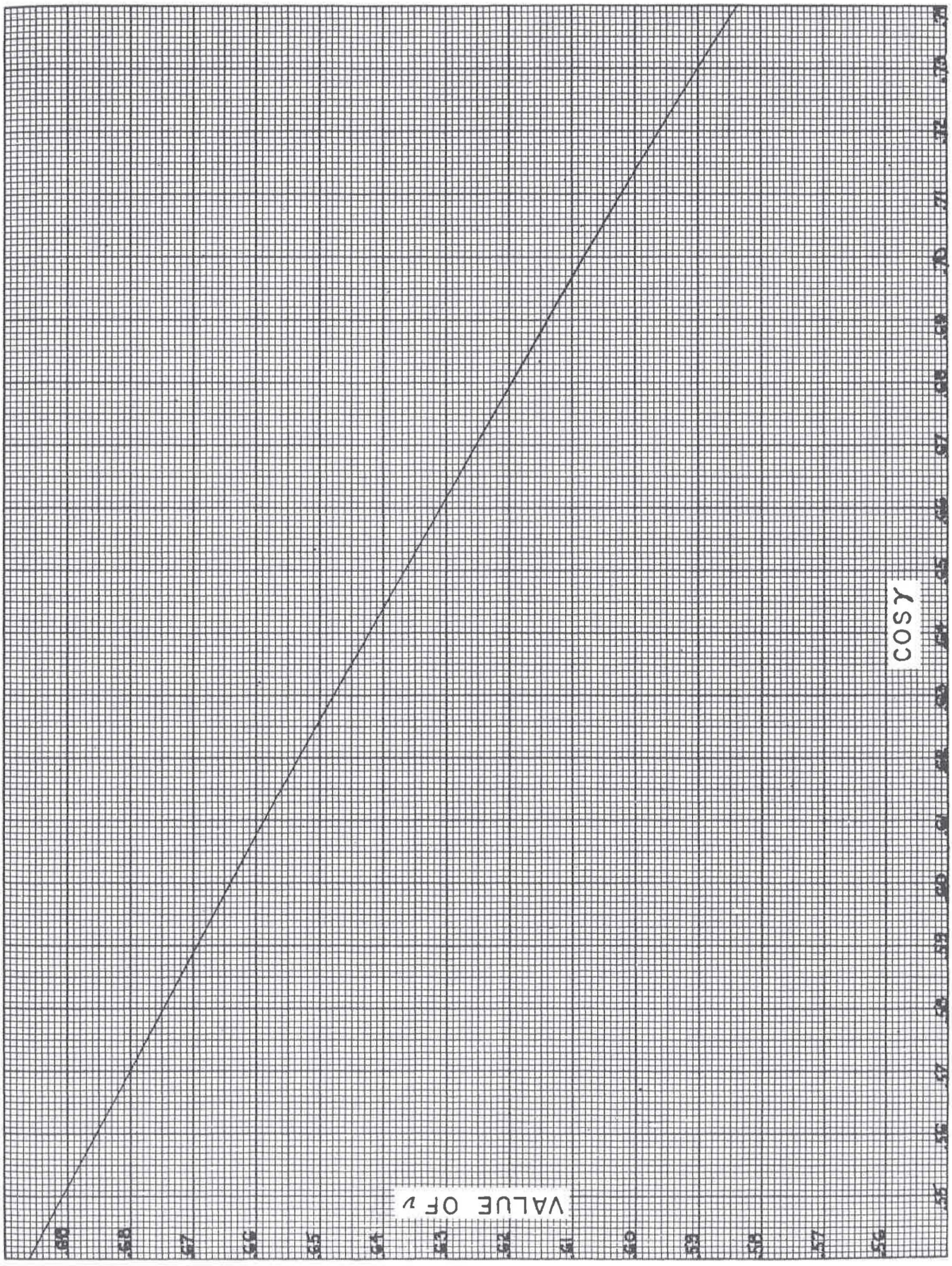


American Axle v. Neapco - IPR2025-00091
PET_AAM_1012-0373

Chart A-20

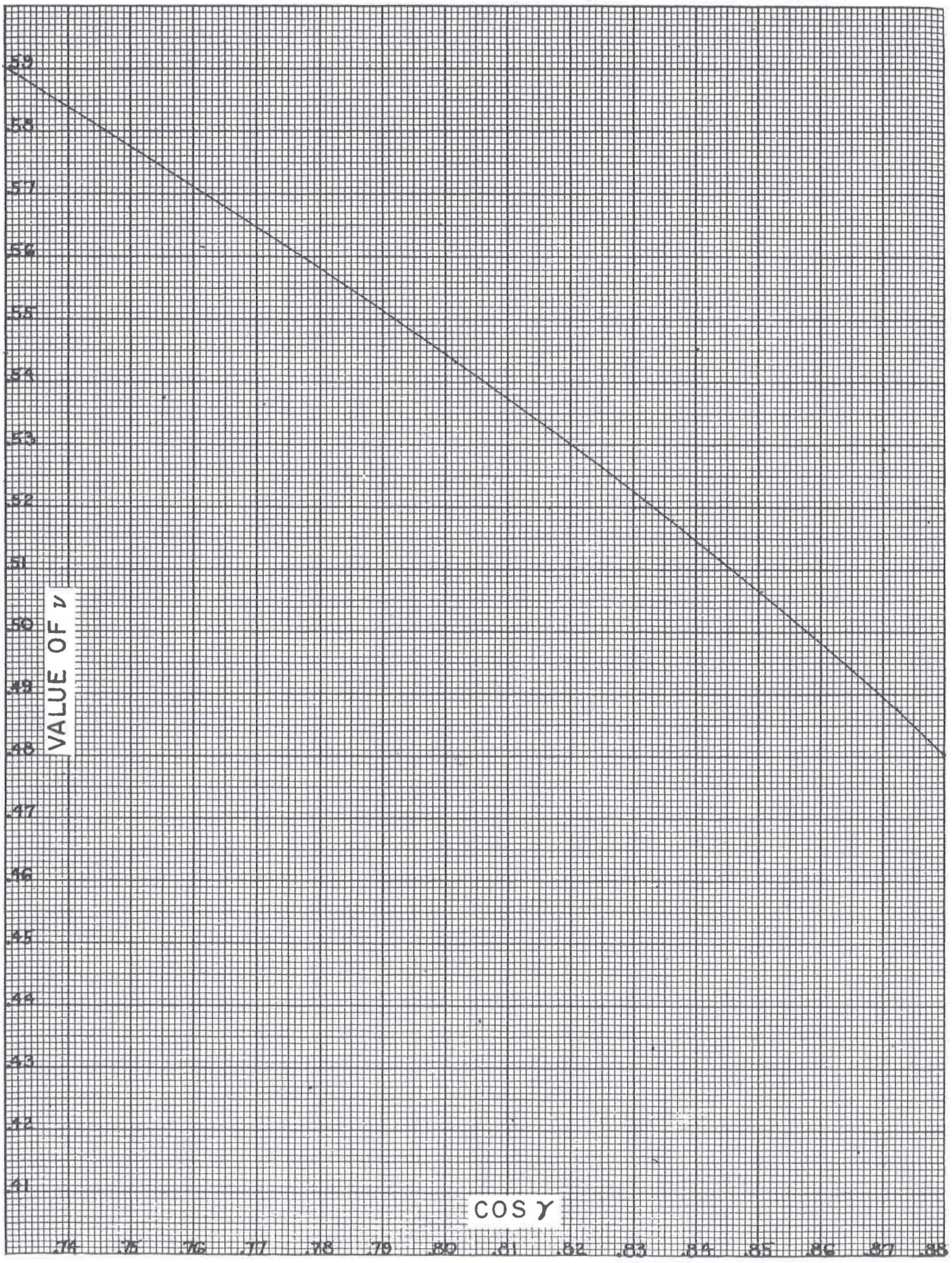


American Axle v. Neapco - IPR2025-00091
PET_AAM_1012-0374

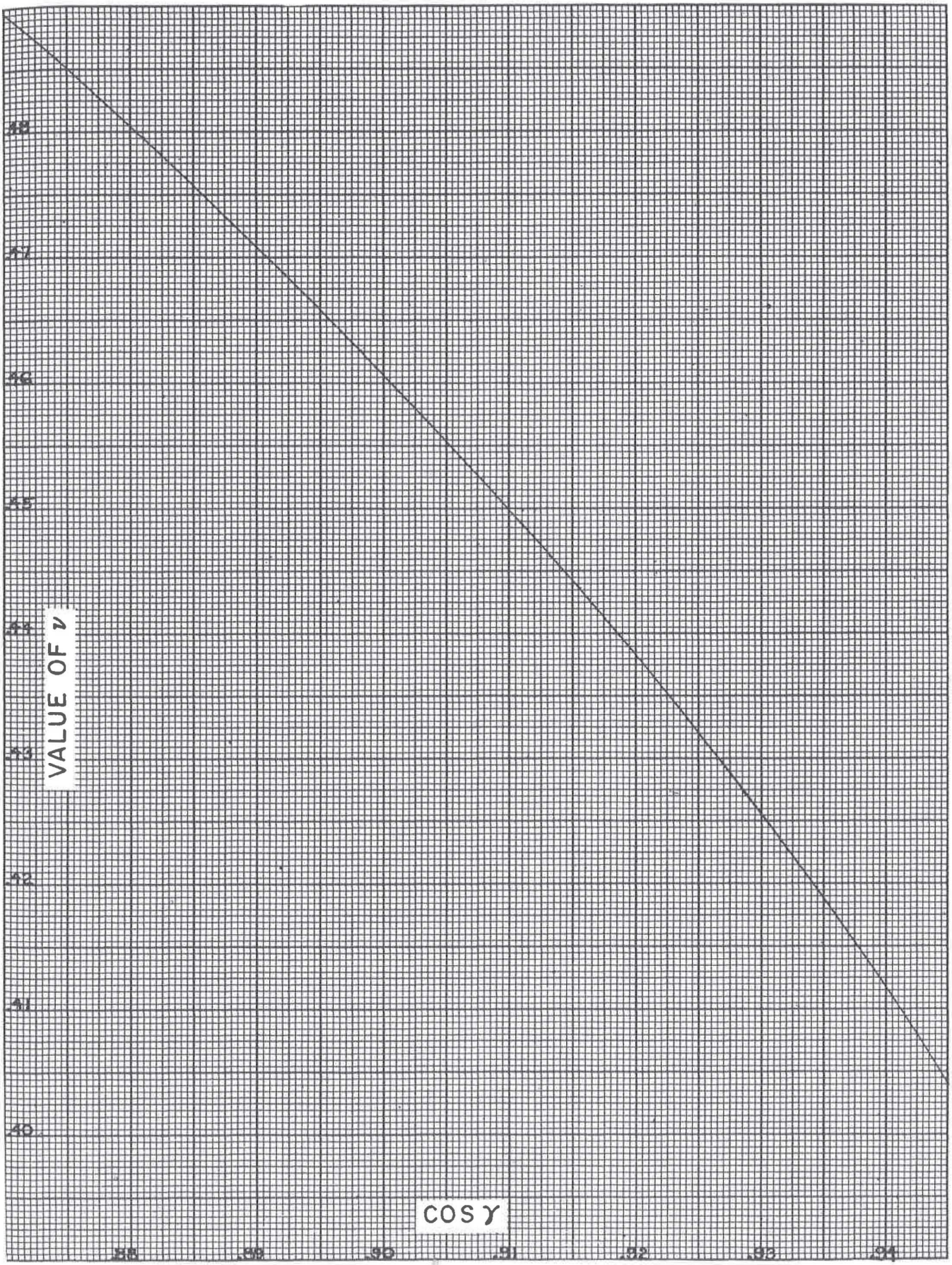


American Axle v. Neapco - IPR2025-00091
PET_AAM_1012-0375

Chart A-22

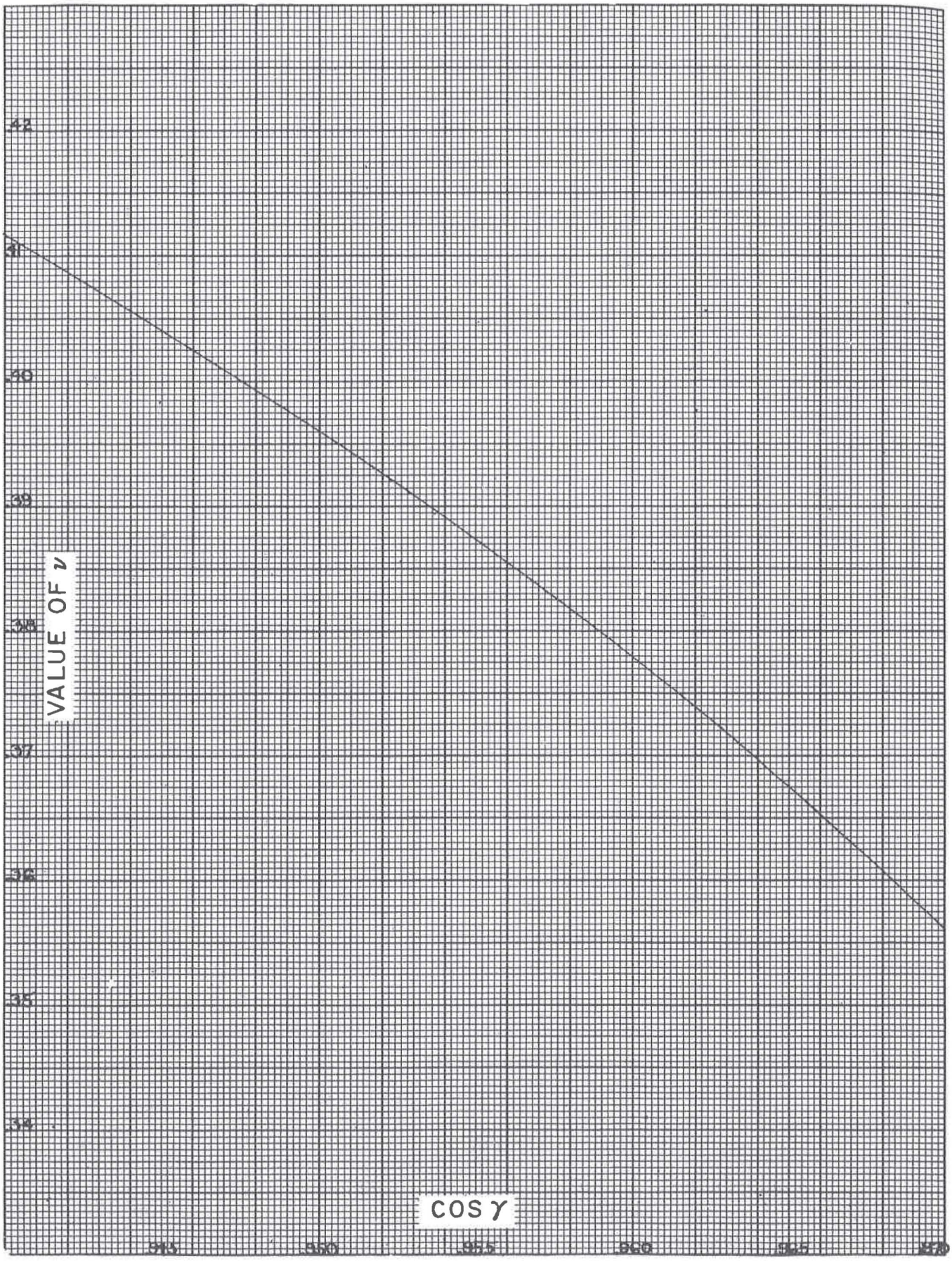


American Axle v. Neapco - IPR2025-00091
PET_AAM_1012-0376



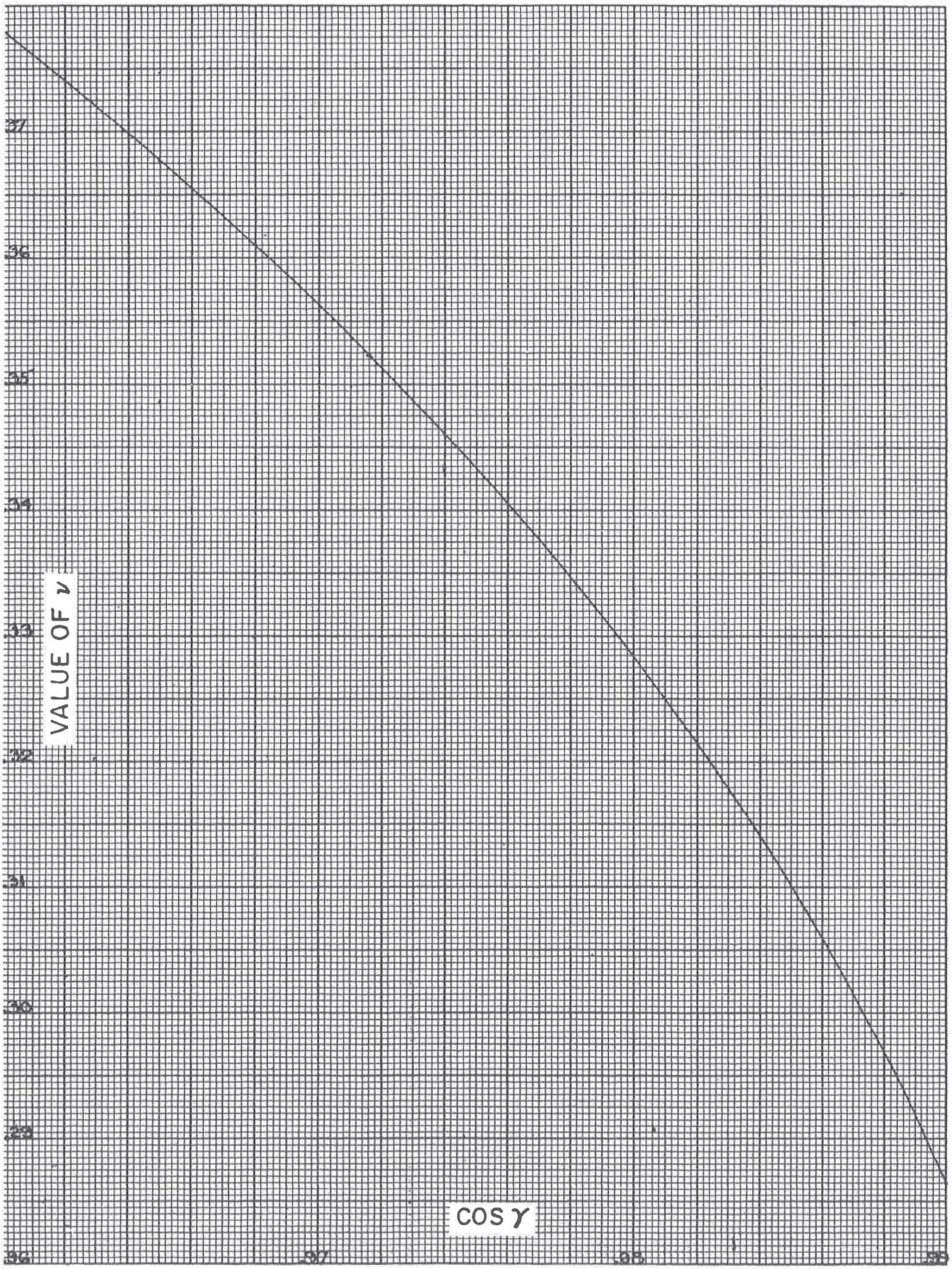
American Axle v. Neapco - IPR2025-00091
PET_AAM_1012-0377

Chart A-24



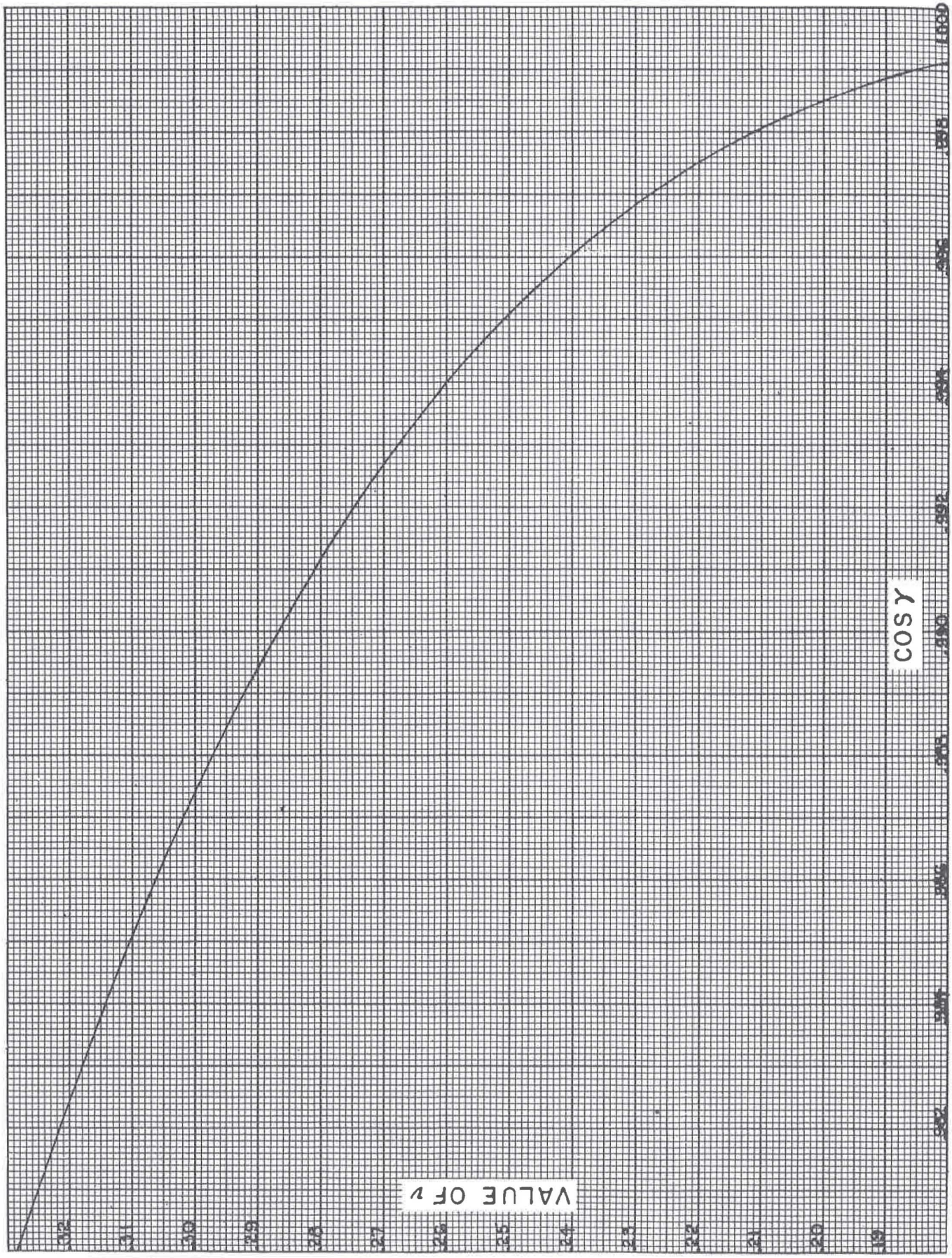
American Axle v. Neapco - IPR2025-00091
PET_AAM_1012-0378

Chart A-25



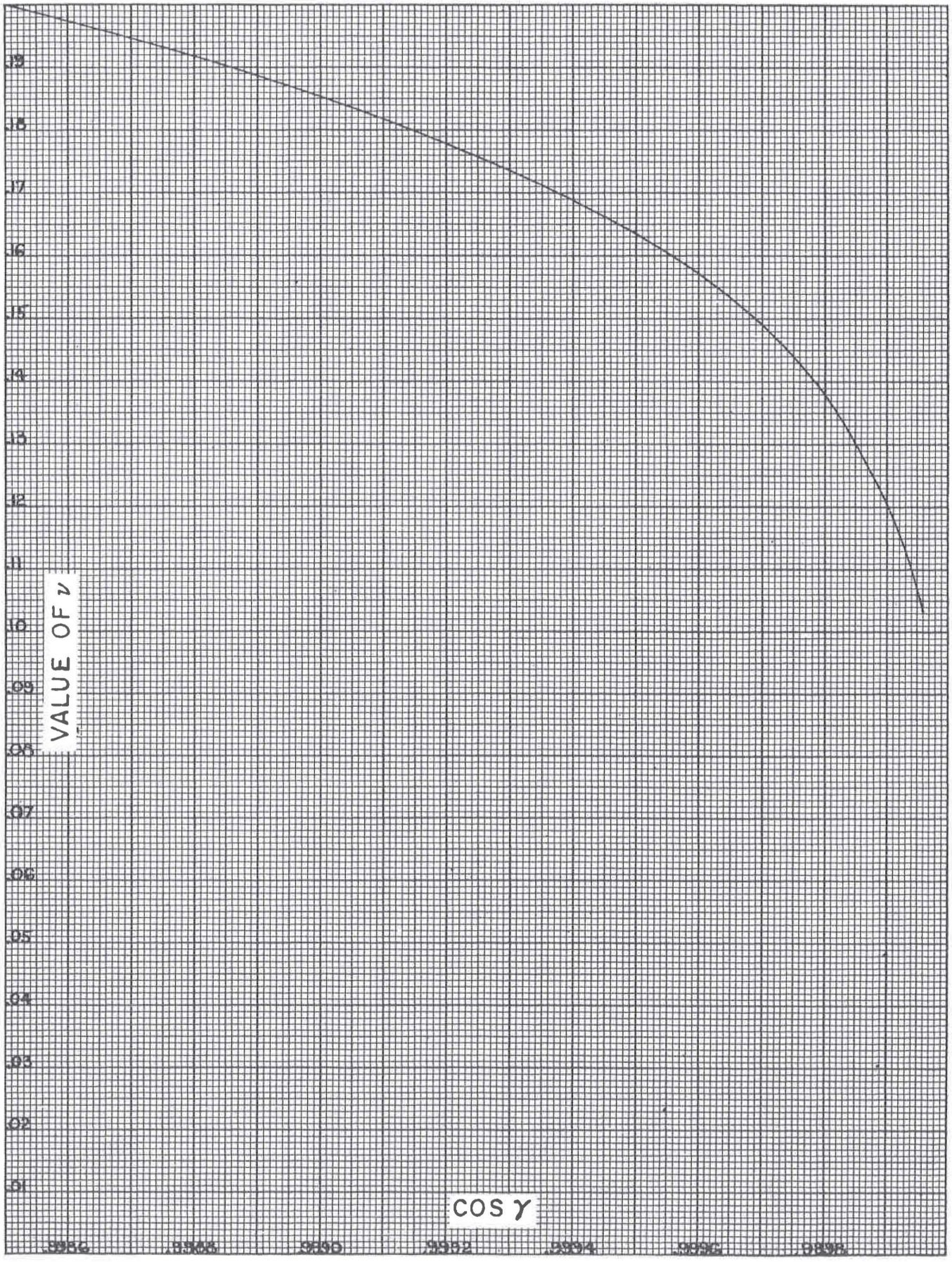
American Axle v. Neapco - IPR2025-00091
PET_AAM_1012-0379

Chart A-26



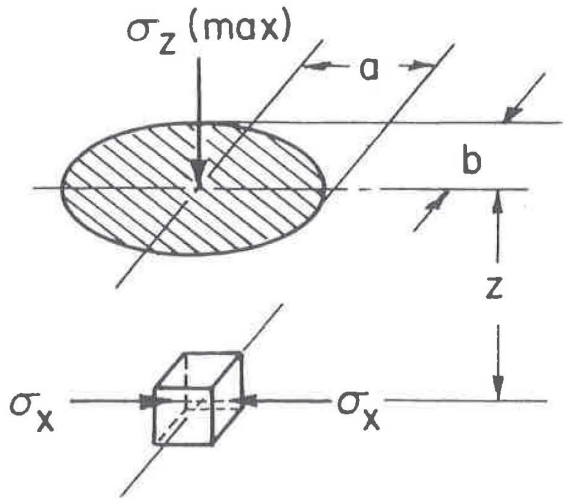
American Axle v. Neapco - IPR2025-00091
PET_AAM_1012-0380

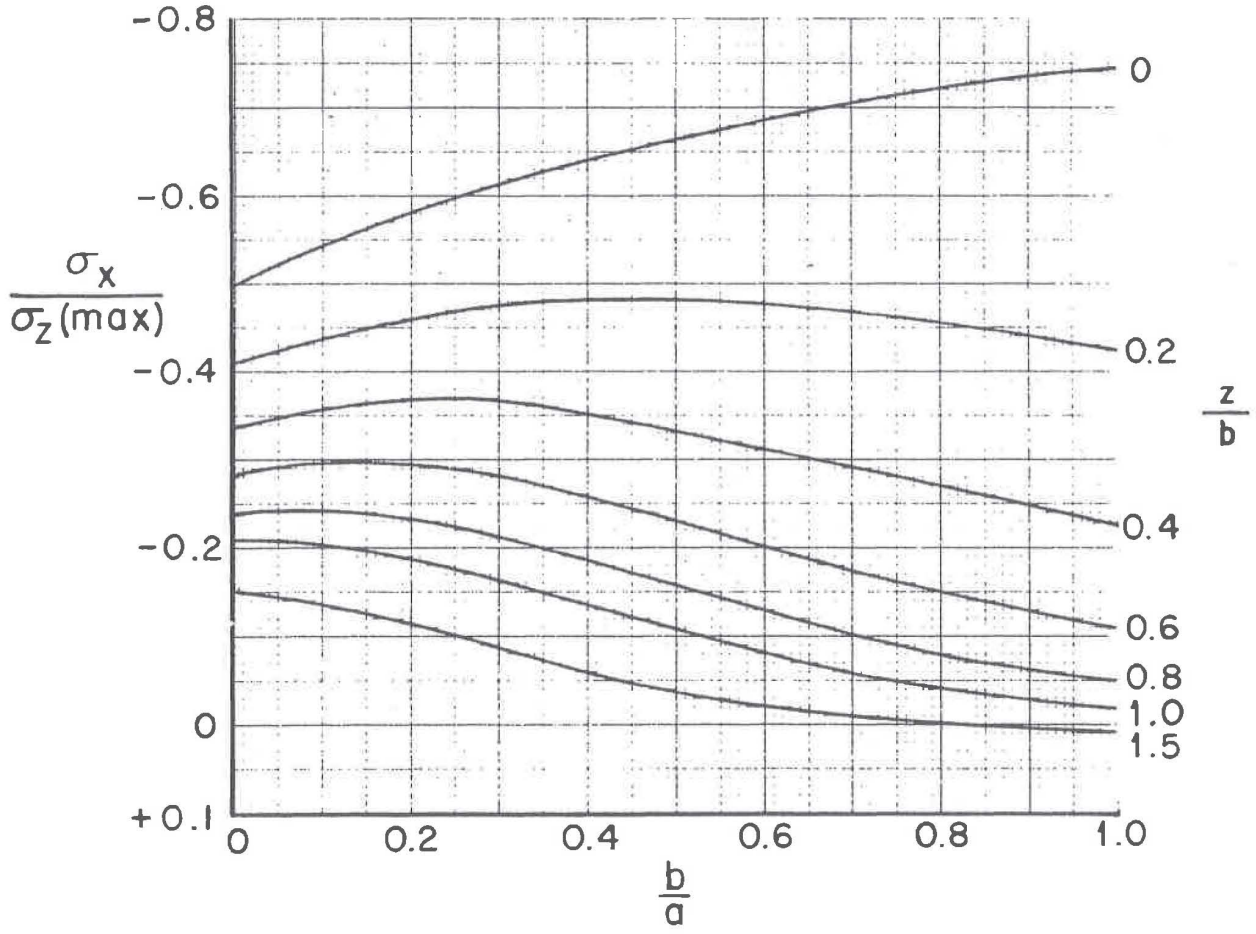
Chart A-27



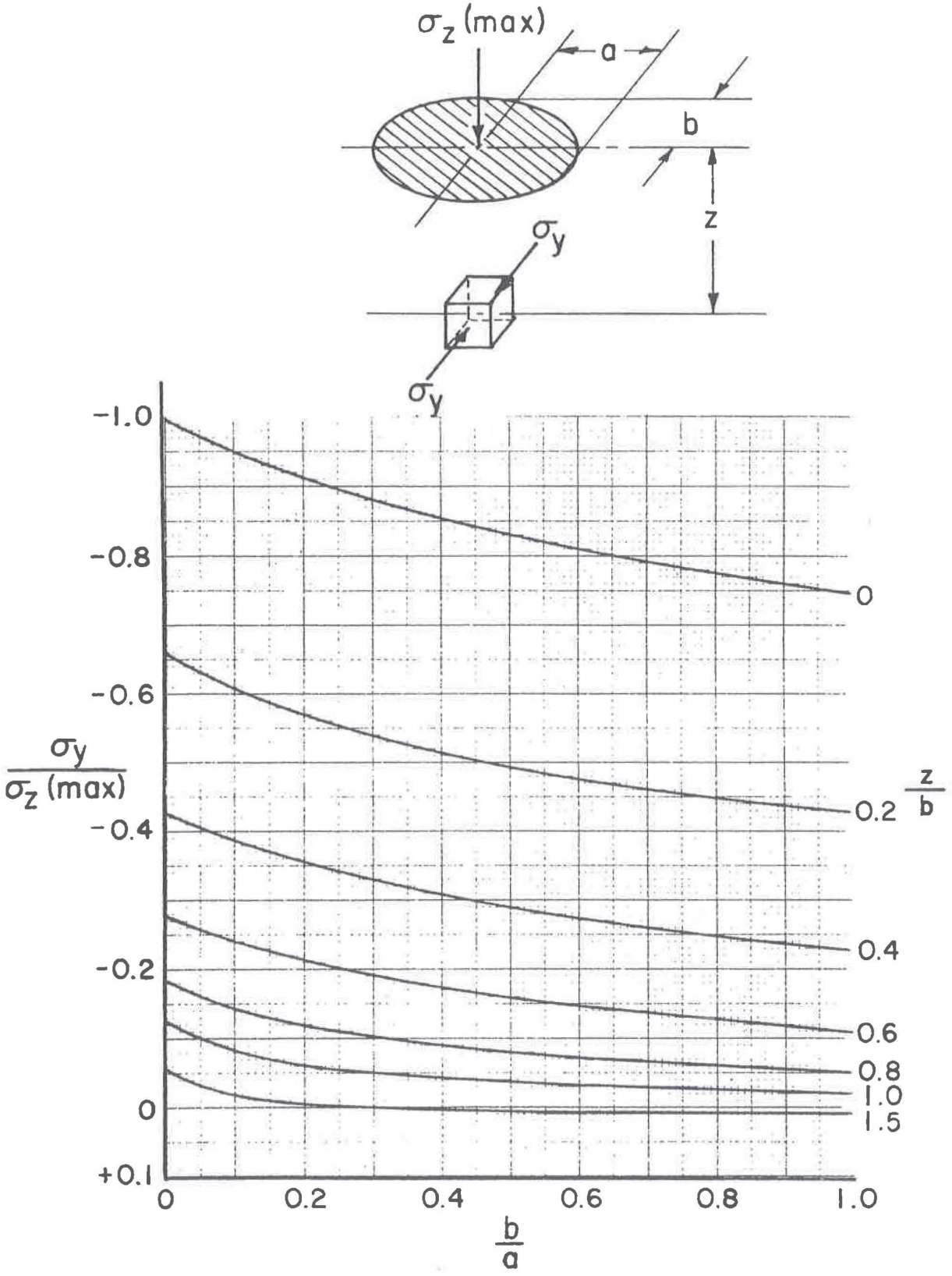
American Axle v. Neapco - IPR2025-00091
PET_AAM_1012-0381

Chart A-28



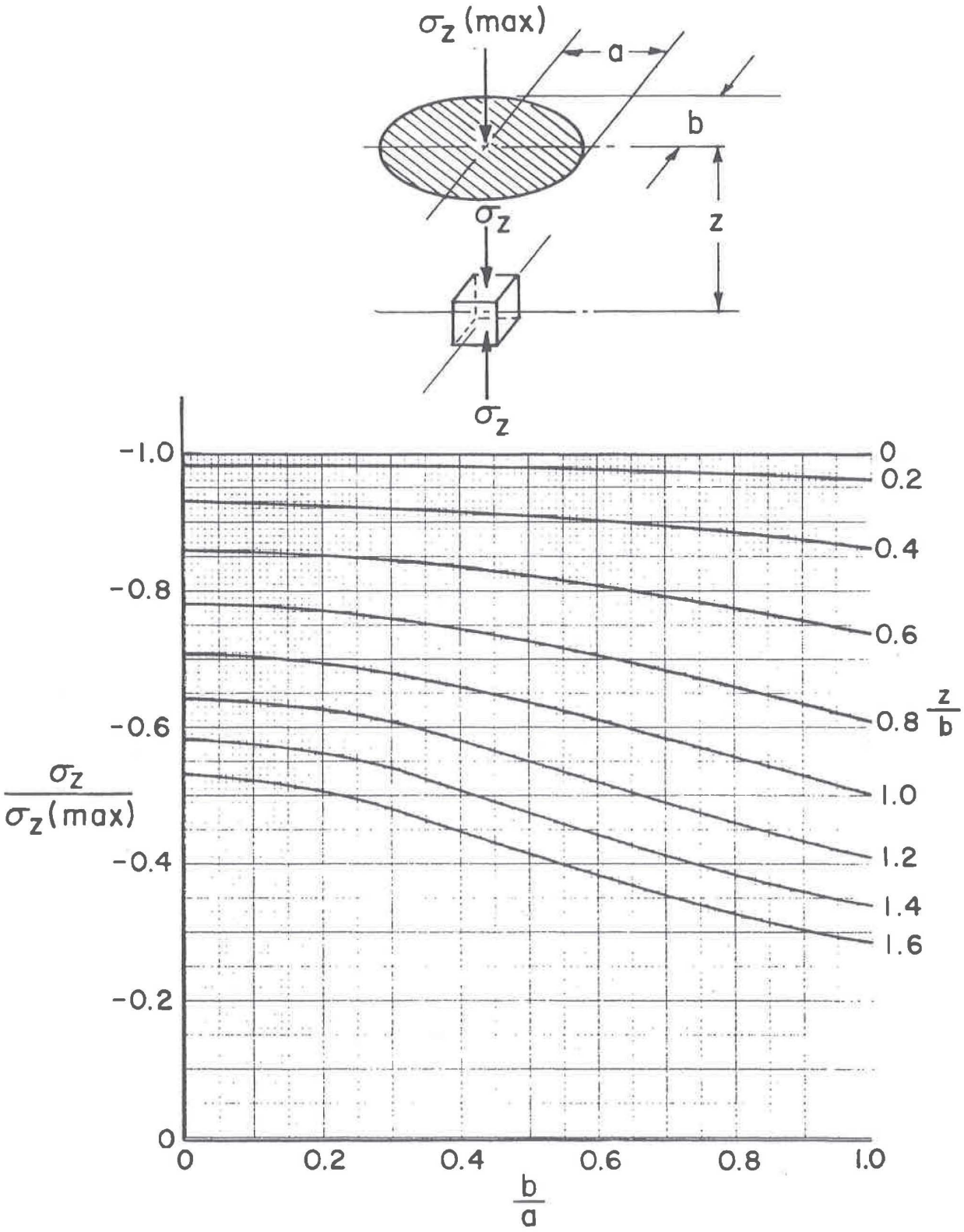


American Axle v. Neapco - IPR2025-00091
PET_AAM_1012-0382



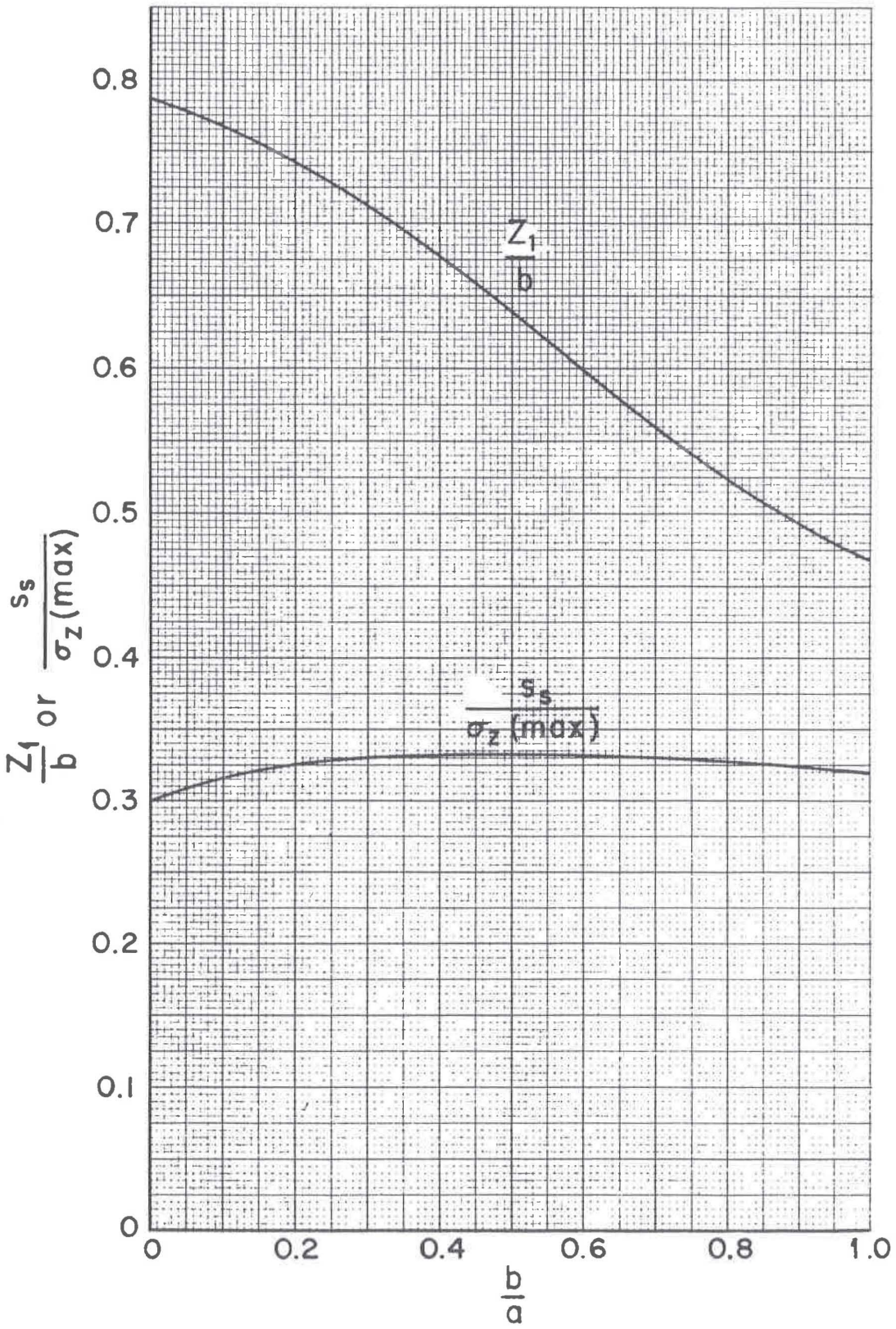
American Axle v. Neapco - IPR2025-00091
PET_AAM_1012-0383

Chart A-30



American Axle v. Neapco - IPR2025-00091
PET_AAM_1012-0384

Chart A-31



American Axle v. Neapco - IPR2025-00091
PET_AAM_1012-0385

APPENDIX B

Basic Load-Speed-Life-Stress Relationships and Equations for Universal Joints with Rolling Elements

E. R. Wagner, P.E. — Saginaw Steering Gear Div., GMC

The basic load-speed-life-stress relationships applicable to rolling element bearings can be useful in design and life computations for universal joints employing similar rolling elements. The life expectancy of a joint is a function of the application requirements such as torque, speed, and joint angle, as well as other factors. Since a universal joint can operate at a fixed joint angle or at varying degrees of angularity in a given application, this important characteristic must be included in determining joint life. For a fixed relationship of these variables, a life expectancy value can be established by laboratory testing, and for this same fixed relationship, the empirically determined life expectancy value will vary with the different types of joints. Therefore, through appropriate testing procedures for a given type of joint, it is possible to establish a useful life chart or charts which can incorporate the effects of torque, speed, and joint angle.

The basic load-speed-life-stress relationships and equations are given in the following Tables, B-1 and B-2, for universal joints with rolling elements consisting of needle rollers or rollers, and with rolling elements consisting of balls.

TABLE B-1 — UNIVERSAL JOINTS WITH NEEDLE ROLLERS OR ROLLERS

Relationship	Equation
$L \propto (\frac{1}{P})^{10/3}$	$L_2 = L_1 (\frac{P_1}{P_2})^{10/3}$
$L \propto \frac{1}{S^6}$	$L_2 = L_1 (\frac{S_1}{S_2})^6$
$L \propto \frac{1}{N}$	$L_2 = L_1 (\frac{N_1}{N_2})$
$S \propto (P)^{1/2}$	$S_2 = S_1 (\frac{P_2}{P_1})^{1/2}$

where:
- L = Life
- P = Load
- N = Speed
- S = Hertz compressive (contact) stress.
- $\propto$ = Proportional

TABLE B-2 — UNIVERSAL JOINTS WITH BALLS

Relationship	Equation
$L \propto (\frac{1}{P})^3$	$L_2 = L_1 (\frac{P_1}{P_2})^3$
$L \propto \frac{1}{S^9}$	$L_2 = L_1 (\frac{S_1}{S_2})^9$
$L \propto \frac{1}{N}$	$L_2 = L_1 (\frac{N_1}{N_2})$
$S \propto (P)^{1/3}$	$S_2 = S_1 (\frac{P_2}{P_1})^{1/3}$

where:
- L = Life
- P = Load
- N = Speed
- S = Hertz compressive (contact) stress
- $\propto$ = Proportional

It is also possible to combine appropriate equations as follows:

$$L_2 = L_1 \left(\frac{N_1}{N_2}\right) \left(\frac{P_1}{P_2}\right)^3$$

American Axle v. Neapco - IPR2025-00091
PET_AAM_1012-0387

APPENDIX C

Needle Roller Bearing Computation Procedure

E. R. Wagner, P.E. — Saginaw Steering Gear Div., GMC

The bearing elements of a typical full complement needle roller bearing are shown in Fig. C-1 with appropriate nomenclature.

Nomenclature

n = Number of rollers per bearing path
c.c. = Total circumferential clearance
P.D. = Pitch diameter
B = Outer raceway or bearing bore diameter
D = Journal or trunnion diameter
d = Roller diameter
d.c. = Diametral clearance
K = Chordal factor, $1/\sin \frac{180°}{n}$ (See Table C-1)

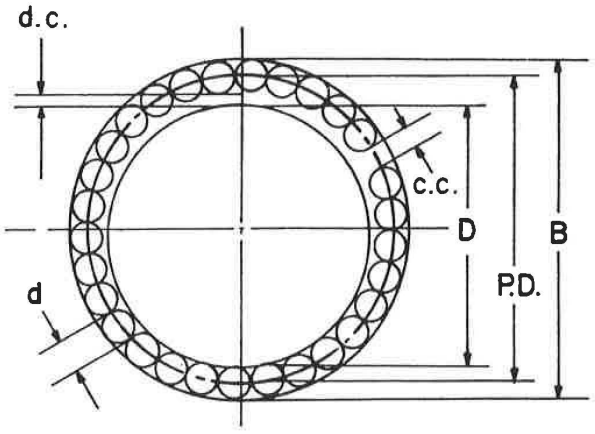


Fig. C-1—Needle roller bearing

Table C–1–K Values (Chordal Factors)

n	K	n	K
6	2.00000	34	10.83795
7	2.30477	35	11.15582
8	2.61313	36	11.47371
9	2.92380	37	11.79163
10	3.23607	38	12.10957
11	3.54947	39	12.42752
12	3.86370	40	12.74550
13	4.17858	41	13.06349
14	4.49395	42	13.38149
15	4.80973	43	13.69951
16	5.12583	44	14.01754
17	5.44219	45	14.33559
18	5.75877	46	14.65365
19	6.07553	47	14.97171
20	6.39245	48	15.28979
21	6.70951	49	15.60788
22	7.02667	50	15.92597
23	7.34394	51	16.24408
24	7.66130	52	16.56219
25	7.97873	53	16.88031
26	8.29623	54	17.19844
27	8.61379	55	17.51657
28	8.93141	56	17.83471
29	9.24907	57	18.15286
30	9.56677	58	18.47101
31	9.88452	59	18.78916
32	10.20230	60	19.10732
33	10.52011		

In general, for a given universal joint application, a minimum journal, trunnion, or pin diameter is required for strength or other design reasons as determined by preliminary computations. Also, it is desirable to select an optimum needle roller size for the bearing.

With this information, it is possible to compute the required number of rollers in the bearing as shown in the following illustrative problem:

$$n = \frac{\pi(D + d)}{d}$$

where:

D = 0.7350 in (minimum trunnion diameter required for strength or other design reasons)
d = 0.0950 in

$$= \frac{\pi(0.7350 + 0.0950)}{0.0950}$$

n = 27.45 needle rollers (say 28 rollers)

Now the actual journal and bore diameters can be computed by using the number of rollers as well as assuming the individual bearing component tolerances and the minimum diametral and circumferential clearances. In addition, the maximum diametral and circumferential clearances can be determined to verify the desired fit-up of the bearing elements.

The following bearing computation procedure can be used.

Assume:
28 needle rollers (0.0950-0.0948 in diameter)
0.0001 in minimum d.c.
0.0004 in minimum cc/π
0.001 in total trunnion diametral tolerance
0.001 in total bearing bore diametral tolerance
1. = d = 0.0950 in maximum
2. = K = 8.93141 (for 28 rollers from Table C-1)

American Axle v. Neapco - IPR2025-00091
PET_AAM_1012-0389

3. = (1) × (2) = 0.0950 × 8.93141 = 0.8485 in
4. = cc/π = 0.0004 in minimum
5. = P.D. = (3) + (4) = 0.8485 + 0.0004 = 0.8489 in minimum
6. = (5) − (1) = 0.8489 − 0.0950 = 0.7539 in
7. = d.c. = 0.0001 in minimum
8. = D = (6) − (7) = 0.7539 − 0.0001 = 0.7538 in maximum
9. = Total trunnion tolerance = 0.001 in
10. = D = (8) − (9) = 0.7538 − 0.001 = 0.7528 in minimum
11. = B = (5) + (1) = 0.8489 + 0.0950 = 0.9439 in minimum
12. = Total bearing bore tolerance = 0.001 in
13. = B = (11) + (12) = 0.9439 + 0.001 = 0.9449 in maximum
14. = d = 0.0948 in minimum
15. = (14) × (2) = 0.0948 × 8.93141 = 0.8467 in
16. = P.D. = (13) − (14) = 0.9449 − 0.0948 = 0.8501 in maximum
17. = cc/π = (16) − (15) = 0.8501 − 0.8467 = 0.0034 in maximum
18. = (16) − (14) = 0.8501 − 0.0948 = 0.7553 in
19. = d.c. = (18) − (10) = 0.7553 − 0.7528 = 0.0025 in maximum

The bearing component dimensions and clearances can be summarized as follows:

$\frac{0.0950}{0.0948}$ in needle roller diameter

$\frac{0.7538}{0.7528}$ in trunnion diameter

$\frac{0.9439}{0.9449}$ in bearing bore diameter

$\frac{0.0001}{0.0025}$ in d.c.

$\frac{0.0004}{0.0034}$ in cc/π or $\frac{0.00126}{0.01068}$ in cc

The chordal factors in Table C-1 of this Appendix and the bearing computation procedure have been adapted from Torrington Bearings Catalog 576 with permission of The Torrington Company.

American Axle v. Neapco - IPR2025-00091
PET_AAM_1012-0390

APPENDIX D
Stress Concentration Factors

E. R. Wagner, P.E. — Saginaw Steering Gear Div., GMC

The subject of stress concentration factors is discussed in great detail in textbooks and handbooks listed in the references. Only a brief explanation of the subject is made here.

The ultimate and yield strength of a component is determined not only by its size and geometry, but also by the type of material used and the heat treatment method employed. Manufacturing processing procedures can further affect component strength. All of these factors can result in increased stresses in hypothetically ideal materials, which are completely homogeneous, isotropic, and elastic. The increase of these stresses can be expressed by the presence of points of stress concentration or stress raisers. Common stress raisers include fillets, grooves, holes, threads, splines, keyways, etc. The maximum stress at a section is customarily determined by first calculating the nominal stress (as if the stress raiser did not exist) and then multiplying this value by a geometric or theoretical stress concentration factor designated K_t. Commonly used values of K_t in bending and torsion are shown in Figs. D-1–D-5. These curves are for round shaft members of various geometric constructions and proportions. Values of K_t for other common stress raisers are shown in the following references.

American Axle v. Neapco - IPR2025-00091
PET_AAM_1012-0391

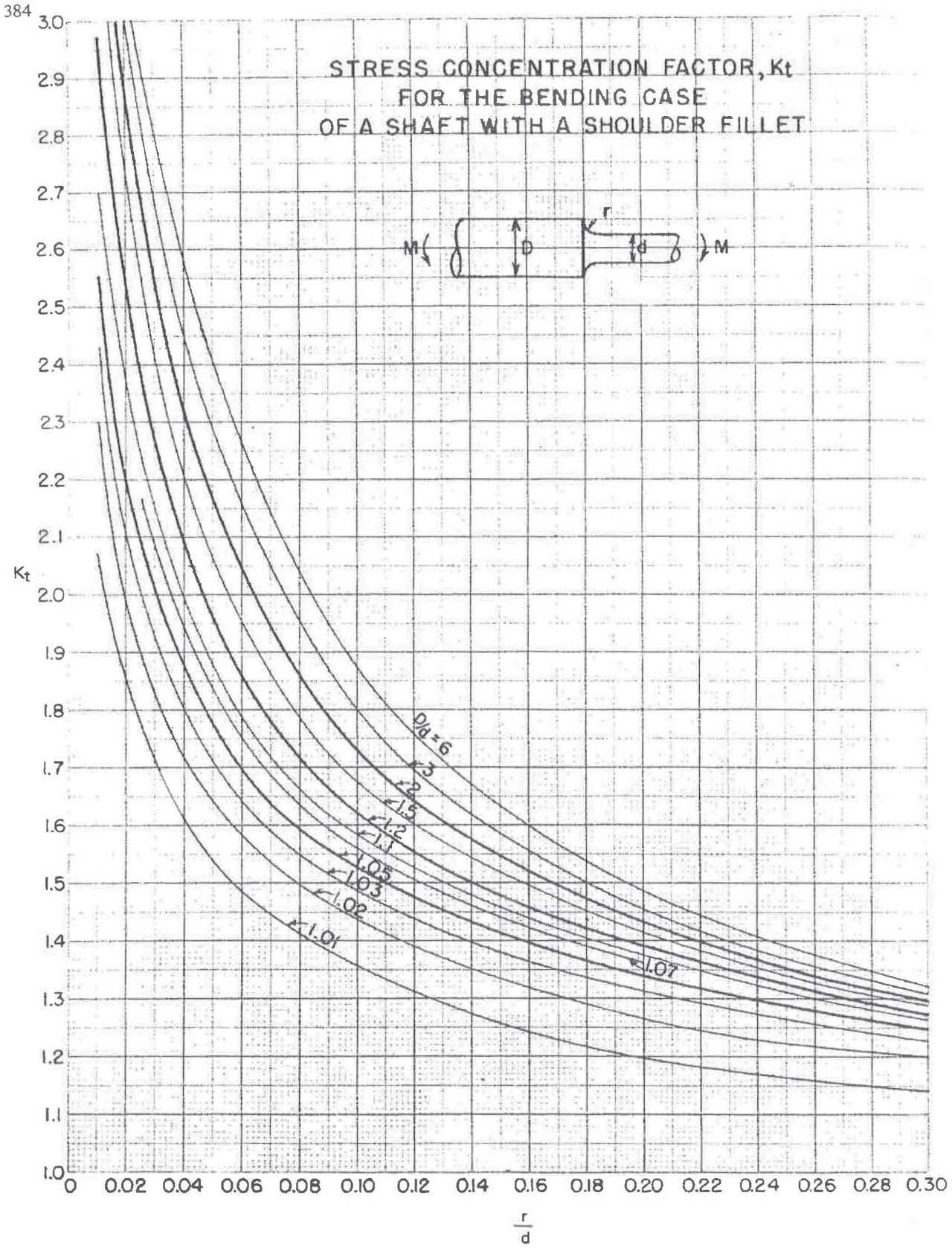


Fig. D-1—Stress concentration factor, K_t for the bending case of a shaft with a shoulder fillet

American Axle v. Neapco - IPR2025-00091
PET_AAM_1012-0392

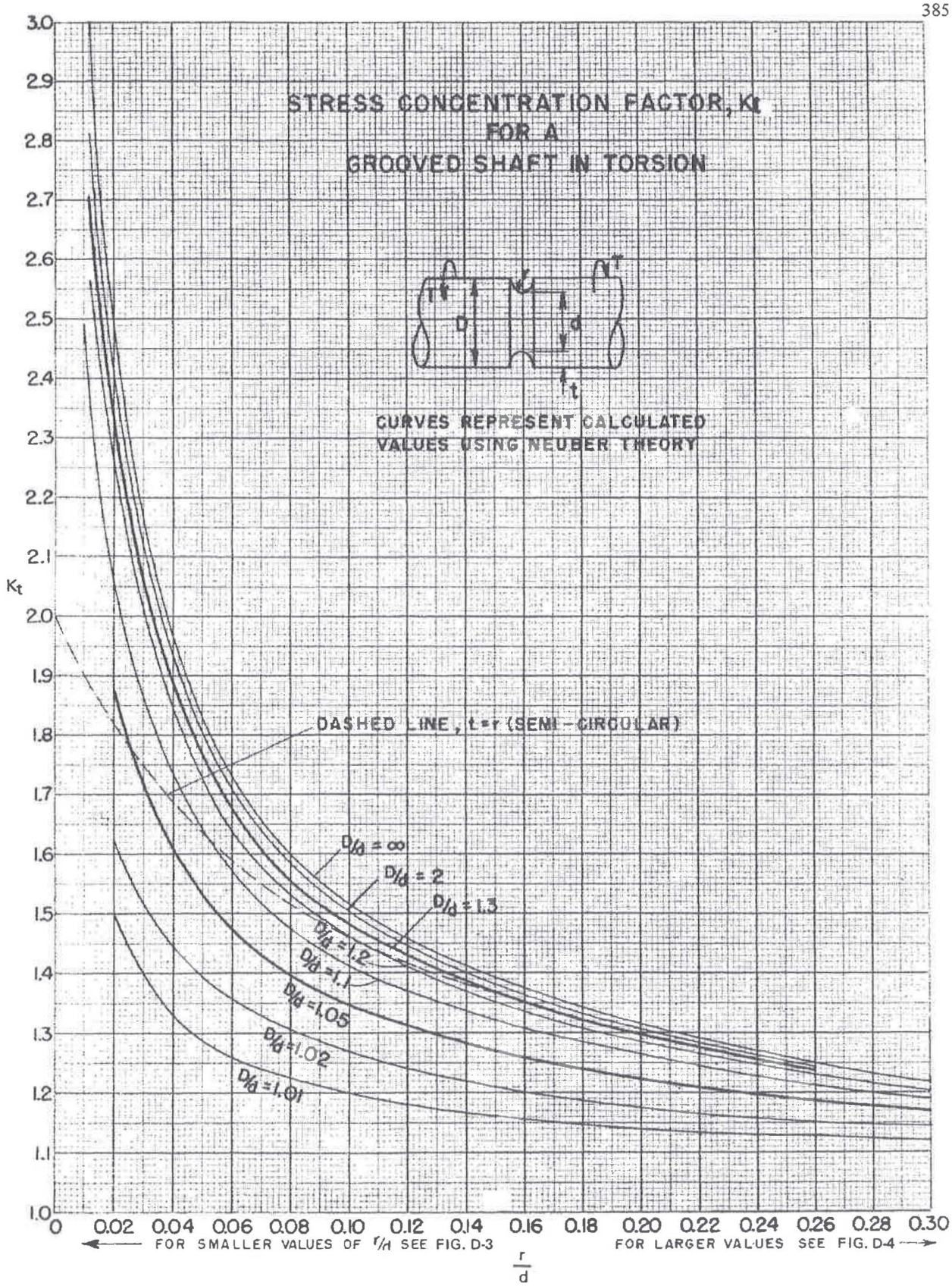


Fig. D-2—Stress concentration factor, K_t for a grooved shaft in torsion

American Axle v. Neapco - IPR2025-00091
PET_AAM_1012-0393

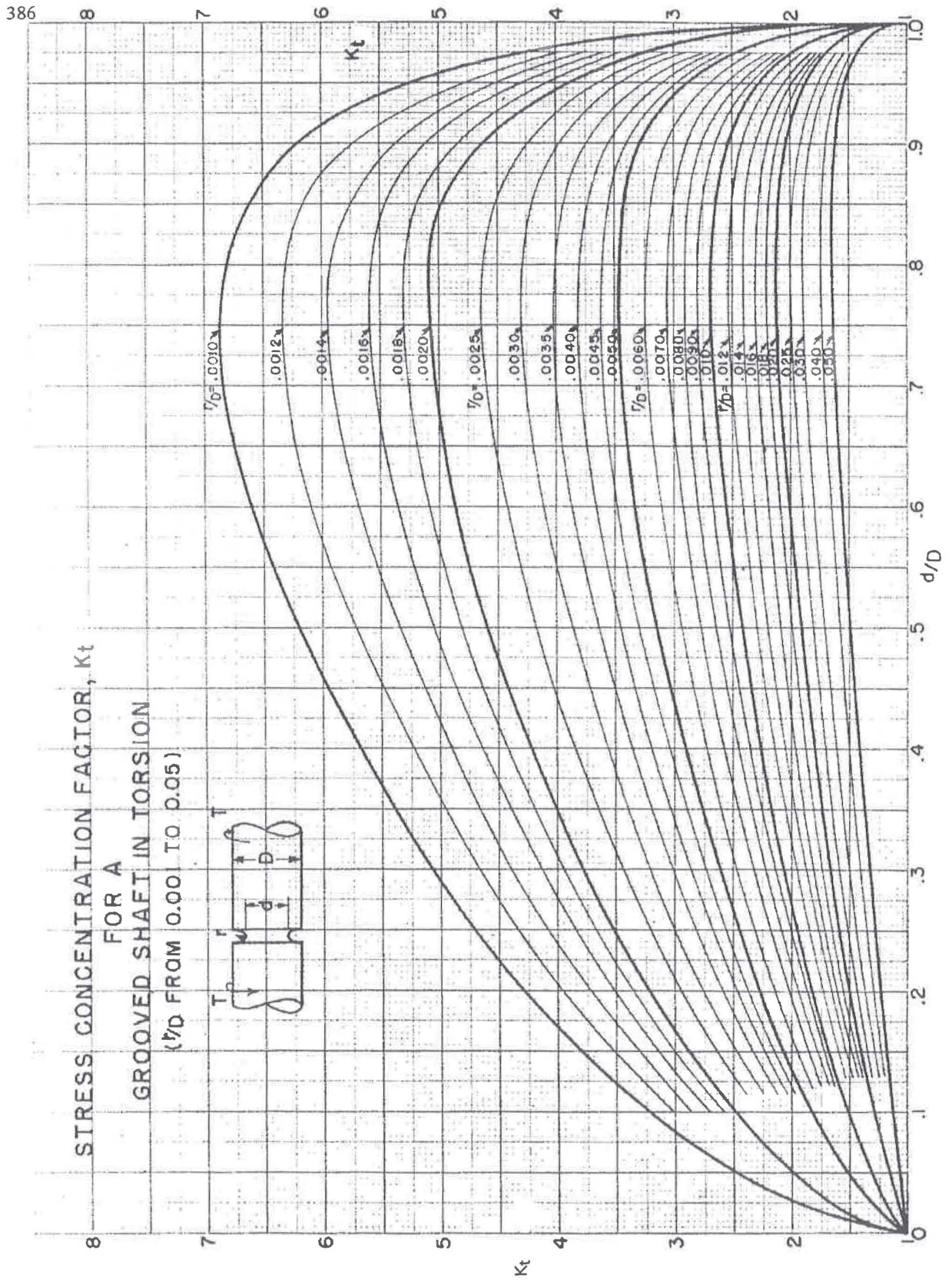


Fig. D-3—Stress concentration factor, K_t for a grooved shaft in torsion

American Axle v. Neapco - IPR2025-00091
PET_AAM_1012-0394

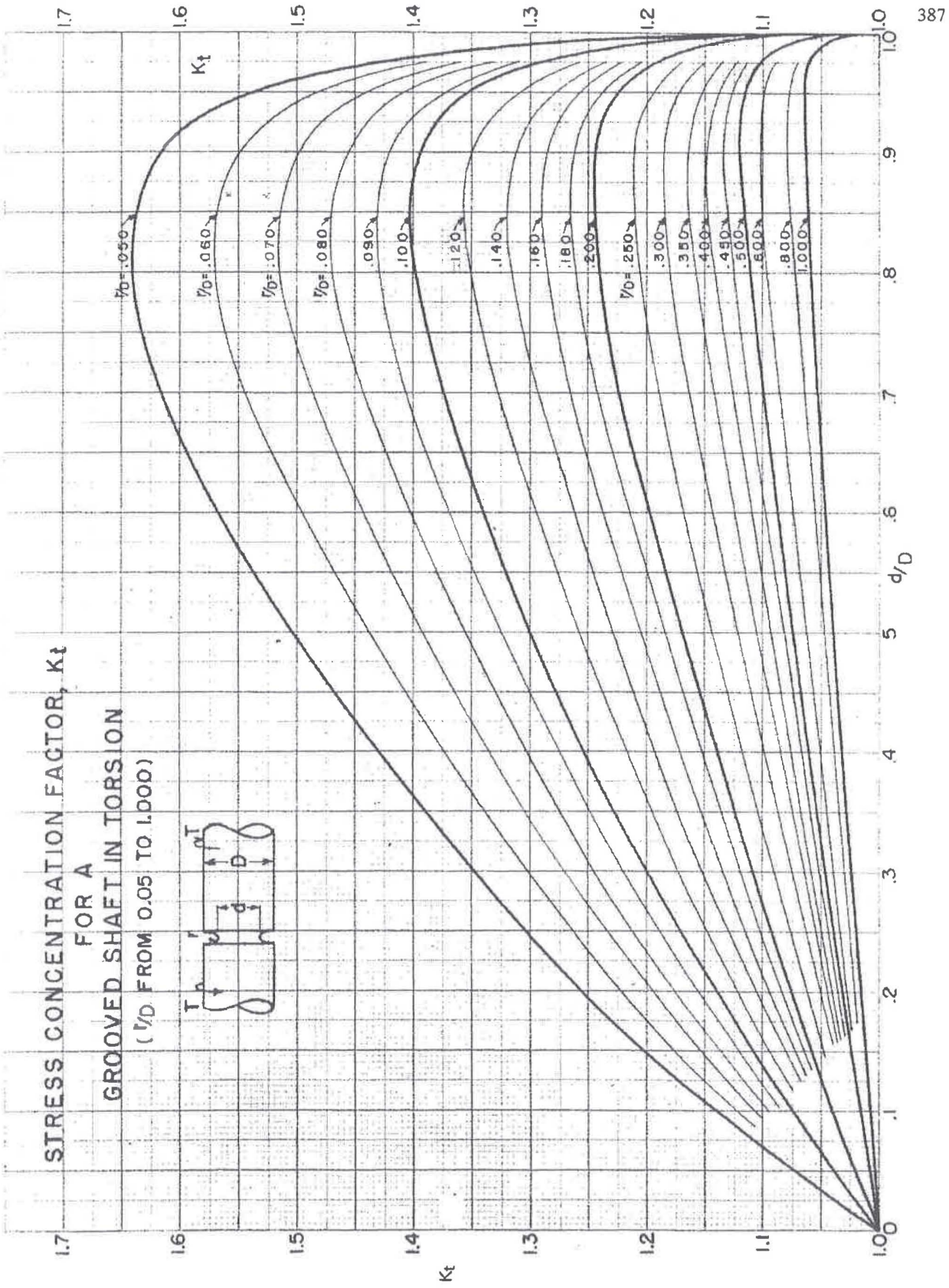


Fig. D-4—Stress concentration factor, K_t for a grooved shaft in torsion

American Axle v. Neapco - IPR2025-00091
PET_AAM_1012-0395

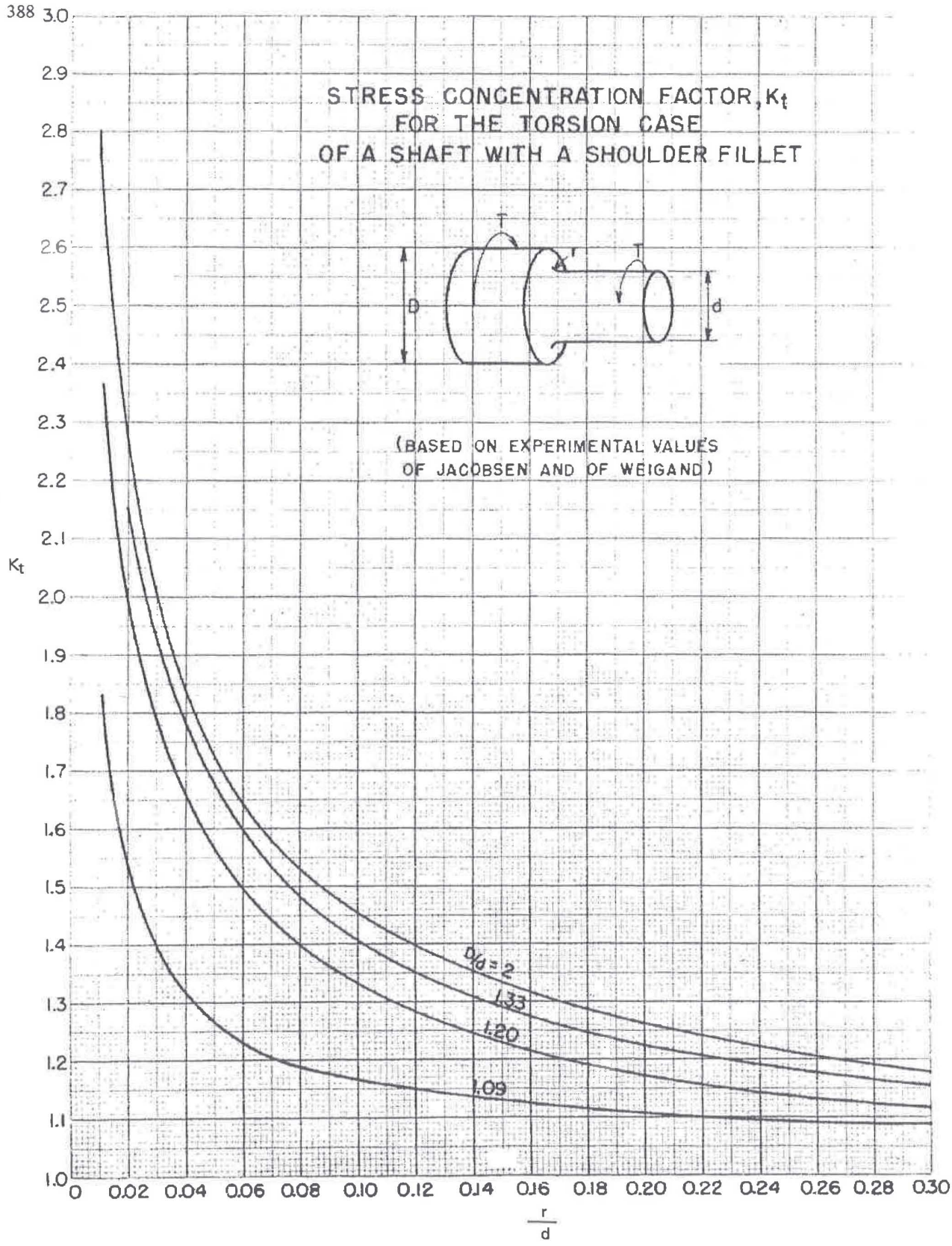


Fig. D-5—Stress concentration factor, K_t for the torsion case of a shaft with a shoulder fillet

American Axle v. Neapco - IPR2025-00091
PET_AAM_1012-0396

References

1. R. E. Peterson, *Stress Concentration Design Factors*. New York: John Wiley and Sons, Inc., 1953.*

2. S. Timoshenko, *Strength of Materials, Part II*. 3rd ed. New Jersey: D. Van Nostrand Co., Inc., 1956.

3. W. Ker Wilson, "Practical Solution of Torsional Vibration Problems," *Strength Calculations*, Vol. 3, 3rd ed. London: Chapman and Hall Ltd., 1965.

4. R. J. Roark, *Formulas for Stress and Strain*. 4th ed. New York: McGraw-Hill Book Co., 1965.

5. R. C. Juvinall, *Engineering Considerations of Stress, Strain, and Strength*. New York: McGraw-Hill Book Co., 1967.

6. *Fatigue Design Handbook*, Society of Automotive Engineers Inc., 1968.

*Stress concentration factors shown in Figs. D-1–D-5 used with the permission of John Wiley and Sons, Inc.

American Axle v. Neapco - IPR2025-00091
PET_AAM_1012-0397

APPENDIX E

Typical Drivetrain Component Efficiencies

E. R. Wagner, P.E. — Saginaw Steering Gear Div., GMC

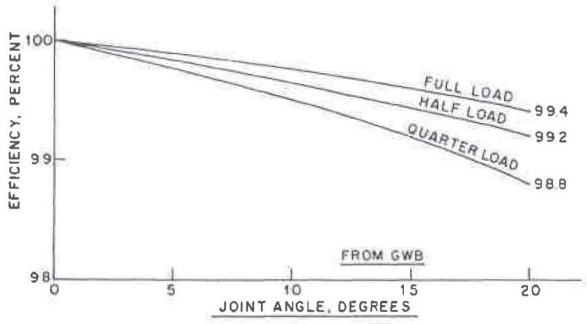


Fig. E-1—Efficiency of driveshaft with two Cardan joints

In driveline computations, efficiencies should be applied as required to correct for losses in the various drivetrain components. Some of these typical customarily used efficiencies are listed in Table E-1.

Table E-1—Drivetrain Component Efficiencies

Drivetrain Component	Efficiency, Percent
Automatic transmission with torque converter	85-90
Manual transmission	90-95
Transfer case	90-95
Auxiliary transmission	90-95
Front or rear axle (single axle)	95
Tandem rear axle	90-95

In certain applications, a knowledge of universal joint efficiency may also be desirable. A typical Cardan universal joint with needle roller bearings has a very high efficiency since power losses primarily due to rolling friction are very small. The power losses are composed of the bearing seal drag and the relative sliding of the bearing and cross thrust surfaces. When the joint angle is increased for a given torque load, the pressure on the bearing thrust faces by the cross trunnion thrust ends becomes greater due to secondary couple action of the joint, thus reducing the efficiency.

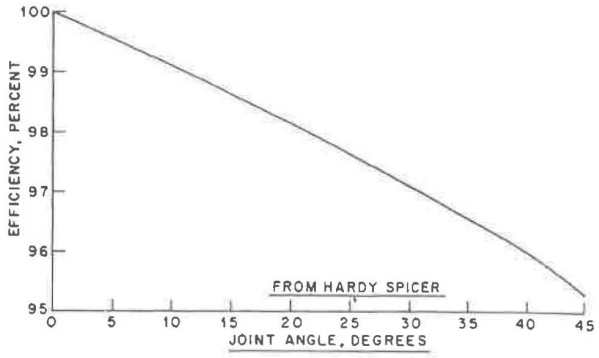


Fig. E-2—Rzeppa joint efficiency

In addition, centrifugal force effects due to unbalance can also increase the force on these thrust surfaces with increasing rotational speeds. The efficiency of a typical driveshaft with two Cardan joints having commonly used parallel or in-line yoke phasing is shown in Fig. E-1 as a function of the joint angle for full load, half load, and quarter load at 3000 rpm. It can be seen that the efficiency is very high and exceeds 99.5% even with only partial load on the driveshaft at up to 10 deg joint angles. Joint angles seldom exceed 10 deg in practice. Therefore, a driveline incorporating Cardan joints with needle roller bearings is a highly efficient drive system.

The efficiency of a typical Rzeppa universal joint is only slightly lower than a Cardan joint because internal losses are low. Losses are caused mainly by internal friction which is affected by ball-to-groove contact geometric characteristics, ball load, relative sliding of the spherical surfaces, rotational speed, and joint angle, and by viscous drag of the lubricant. This viscous drag is determined by the type of lubricant selected and the surrounding conditions affecting heat dissipation from the joint. Fig. E-2 shows the effect of joint angle on the efficiency of a typical Rzeppa joint.

American Axle v. Neapco - IPR2025-00091
PET_AAM_1012-0399